A sequence-based survey of the complex structural organization of tumor genomes

Benjamin J. Raphael[1*], Stanislav Volik[2*], Peng Yu[3], Chunxiao Wu[4], Guiqing Huang[2], Elena V. Linardopoulou[5], Barbara J. Trask[5], Frederic Waldman[2], Joseph Costello[2], Kenneth J. Pienta[6], Gordon B. Mills[7], Krystyna Bajsarowicz[2], Yasuko Kobayashi[2], Shivaranjani Sridharan[2], Pamela Paris[2], Quanzhou Tao[8], Sarah J. Aerni[9], Raymond P. Brown[10], Ali Bashir[10], Joe W. Gray[11], Jan-Fang Cheng[12], Pieter de Jong[13], Mikhail Nefedov[13], Thomas Ried[14], Hesed M. Padilla-Nash[14] and Colin C. Collins[2#].

[1]Department of Computer Science & Center for Computational Molecular Biology, Brown University, 115 Waterman Street, Providence, RI 02912-1910.

[2]Cancer Research Institute, UCSF Comprehensive Cancer Center, 2340 Sutter St. San Francisco, California 94115

[3]Chinese National Human Genome Center, Beijing, China, 100016

[4]Shandong Provincial Hospital, Jinan, China 250021

[5] Division of Human Biology, Fred Hutchinson Cancer Research Center, 1100 Fairview Ave. N., Seattle WA 98109

[6]The University of Michigan, Departments of Internal Medicine and Urology, 1500 E. Medical Center Dr., Ann Arbor, MI 48109-0330

[7]M.D. Anderson Cancer Center, University of Texas, 1515 Holcombe Blvd, Box 0184, Houston, TX 77030

[8]Amplicon Express, 1610 NE Eastgate Blvd. # 880, Pullman, WA 99163 USA

[9]BioMedical Informatics Program, Stanford University, Stanford, CA 94305

[10]Bioinformatics Program, University of California, San Diego, 9500 Gilman Drive, La Jolla, CA 92093

[11]Lawrence Berkeley National Laboratory, Life Sciences Division, One Cyclotron Road, MS 84R171 Berkeley, CA 94720-8268

[12]Lawrence Berkeley National Laboratory, Genomics Division and Joint Genome Institute, One Cyclotron Road, MS 84R171 Berkeley, CA 94720

[13]BACPAC resources Children's Hospital Oakland 747 52nd St. Oakland, CA. 94609

[14]Section of Cancer Genomics, Genetics Branch, Center for Cancer Research, National Cancer Institute, National Inst of Health Bethesda, MD 20892.

*Equal contribution

#Correspondence: collins@cc.ucsf.edu

Abstract

Background: The genomes of many epithelial tumors exhibit extensive chromosomal rearrangements. All classes of genome rearrangements can be identified using End Sequencing Profiling (ESP), which relies on paired-end sequencing of cloned tumor genomes.

Results: In this study, brain, breast, ovary and prostate tumors along with three breast cancer cell lines were surveyed with ESP yielding the largest available collection of sequence-ready tumor genome breakpoints and providing evidence that some rearrangements may be recurrent. Sequencing and fluorescence *in situ* hybridization (FISH) confirmed translocations and complex tumor genome structures that include co-amplification and packaging of disparate genomic loci with associated molecular heterogeneity. Comparison of the tumor genomes suggests recurrent rearrangements. Some are likely to be novel structural polymorphisms, whereas others may be bona fide somatic rearrangements. A recurrent fusion transcript in breast tumors and a constitutional fusion transcript resulting from a segmental duplication were identified. Analysis of end sequences for single nucleotide polymorphisms (SNPs) revealed candidate somatic mutations and an elevated rate of novel SNPs in an ovarian tumor.

Conclusion: These results suggest that the genomes of many epithelial tumors may be far more dynamic and complex than previously appreciated and that genomic fusions including fusion transcripts and proteins may be common, possibly yielding tumor-specific biomarkers and therapeutic targets.

Background

Cancer is driven by selection for certain somatic mutations including both point mutations and large-scale rearrangements of the genome; thus, the genomes of most human solid tumors are substantially diverged from the host genome. Many copy number aberrations have been shown to be recurrent across multiple cancer samples. These recurrent copy number aberrations frequently contain oncogenes and tumor suppressor genes and are associated with tumor progression, clinical course, or response to therapy [1]. Moreover, it is now possible to alter the clinical course of breast cancer by the therapeutic targeting of amplified ERBB2 oncoprotein [2].

Structural rearrangements, particularly translocations, are frequently observed in solid and hematopoietic tumors. In hematopoietic malignancies the importance of translocations is well established, but their biological and clinical significance in solid tumors remains largely enigmatic due to technical difficulties and complex karyotypes that defy interpretation. Recently, a bioinformatics approach identified recurrent translocations in ~50% of prostate tumors [3]. This discovery of recurrent translocations in prostate tumors is important because it demonstrates their presence in a common solid tumor and may make possible development of *tumor-specific* biomarkers and drug targets. Therapeutics such as Gleevec that are directed toward tumor-specific molecules may be more efficacious with fewer off-target effects than therapies aimed at molecules whose structures and/or expression are not tumor-specific.

End Sequencing Profiling (ESP) is a technique that maps and clones all types of rearrangements while generating reagents for functional studies [4-7]. To perform ESP using bacterial artificial chromosomes (BACs), a BAC library is constructed from tumor DNA, BACs are end sequenced, and the end sequences aligned to the reference human genome sequence (

Figure 1). Previous ESP analysis of the breast cancer cell line MCF7 revealed numerous rearrangements and evidence of co-amplification and co-localization of multiple noncontiguous loci [6, 7]. Similarly complex tumor genome structures were recently identified in cell lines derived from breast, metastatic small cell lung, lung neuroendocrine tumor using BAC end sequencing [8].

We performed ESP on: one sample each of primary tumors of the brain, breast, ovary; one metastatic prostate tumor; and two breast cancer cell lines, BT474 and SKBR3. Hundreds of rearrangements were identified in each sample, some of which may encode fusion genes. Fluorescence *in situ* hybridization (FISH) confirmed the presence of translocations predicted by ESP in BT474 and SKBR3. Sequencing of 41 BAC clones from cell lines and primary tumors validated a total 90 rearrangement breakpoints. Mapping these breakpoints in multiple breakpoint spanning clones provided evidence of numerous genomic rearrangements that share similar but not identical breakpoints, a phenomenon analogous to the inter-patient variability of breakpoint locations in many fusion genes identified in haematopoietic cancers. Comparison of rearrangements shared across multiple tumors and/or cell lines suggests recurrent rearrangements, some of which confirm or suggest new germline structural variants, while others may be recurrent somatic variants. Analysis of single nucleotide polymorphisms (SNPs) in BAC end

sequences revealed putative somatic mutations and suggests a higher mutation rate in the ovarian tumor.

ESP complements other strategies for tumor genome analysis including array comparative genomic hybridization (aCGH) and exon resequencing by providing structural information that is otherwise not available. New sequencing technologies [9] promise to radically decrease the cost of ESP and thus make it widely applicable for analysis of hundreds to thousands of tumor specimens at unprecedented resolution. The current study previews the discoveries of such future large-scale studies, examines some of the challenges these studies will face, and provides reagents (genomic clones) for further functional studies, particularly for cell lines which have proved useful as models for cancer research [10, 11].

Results

Tumor BAC libraries

Bacterial artificial chromosome (BAC) libraries were constructed from frozen samples from two breast tumors and single tumors from the brain, ovary and prostate, demonstrating that there is no tumor-specific bias for BAC library construction. Approximately 50 mg to 200 mg of fresh frozen tumor specimen was used in the construction of each library. All tumors were dissected to minimize contamination with normal tissue. BAC libraries from the breast cancer cell lines BT474 and SKBR3 were also constructed. Breast cancer cell lines were included in this study because their genomes and transcriptomes are similar to those identified in primary breast [10, 11] and are invaluable for functional studies. BT474 and SKBR3 were chosen because their aCGH profiles are similar to the profile of previously studied MCF7 cell line [6, 7]. All three cell lines have very high amplifications at the *ZNF217* locus on 20q13 and very high amplifications at chromosome 17. Table 1 lists the clinical characteristics of the tumors and properties of the BAC libraries.

BAC end sequencing and mapping

End sequences of 4,198 BAC clones from the brain tumor library, 5,013 clones from the metastatic prostate library, 5,570 clones from ovary tumor library, 9,401 and 7,623 clones each from primary breast libraries, 9,580 clones from the BT474 and 9,267 clones from the SKBR3 breast cancer cell lines were generated. The end sequences (59.7Mb in total) were mapped to the reference human genome sequence, and the results are summarized in Table 2. We analyzed end sequences that mapped uniquely to the reference sequence, excluding those in repetitive regions, segmental duplications, or duplication-rich centromeric and subtelomeric regions. The density of mapped end sequences in ESP closely matched copy number profiles generated using tiling path BAC arrays [6]. Outside these regions, the distribution of mapped end sequences along the genome did not display other significant gaps or high density arguing against any unusual cloning bias or mapping artifacts. For comparison and further analysis, we included 29.7Mb of sequence from 19,831 end sequenced clones from MCF7 and 701 end sequenced clones from a normal human library (K0241) previously reported [7].

Each clone with uniquely mapped ends gives a *BAC end sequence pair* (BES *pair*). A BES pair is a *valid pair* if distance between ends mapped on the normal human genome sequence and the orientation of these ends and are consistent with those for a BAC clone insert; otherwise, the BES pair is *invalid* (Figure 1). An invalid pair indicates a BAC clone that may span a genomic rearrangement. These are relatively rare, comprising 2.1-4.3% of the mapped BES pairs (Table 2 and Table S1 in Additional data file 1). The largest fractions of invalid pairs are observed in the three breast cancer cell lines, with the greatest (4.3%) observed in MCF7. The majority of these invalid pairs map to amplicons known to co-localize with other loci. DNA within these structures is highly rearranged [4-7]. Among the primary tumors, the greatest fraction of invalid pairs is in the prostate metastasis library (Table 1).

For each library, we formed *BES clusters* grouping invalid pairs with close locations and identical orientations that are consistent with the same genome rearrangement [4]. Each BES cluster provided evidence that the inferred rearrangements are not experimental artifacts. We identified numerous BES clusters in each tumor (Table 2). The fraction of end-sequenced clones that lie in clusters is much lower for clinical tumor samples than cell lines, possibly due to the lower sequence coverage, normal tissue admixture, or greater genomic heterogeneity in the primary tumors. Moreover, the coverage of the genome by valid pairs was significantly lower than either predicted by Lander-Waterman statistics or obtained by modeling using matched *in silico* BAC libraries [See Additional data file 1 and Figures S1 and S2 in Additional data file 2]. This apparent reduction in coverage is likely a result of differing amounts of aneuploidy and genomic heterogeneity in the samples.

Sequencing rearrangement breakpoints

We performed low coverage sequencing of 37 BAC clones corresponding to invalid BES pairs and combined this data with 10 previously sequenced MCF7 BACs [7]. For each BAC, 96 3-kb subclones were end-sequenced, and subclones spanning the breakpoints identified. These subclones were then sequenced to pinpoint the breakpoints more precisely. This procedure identified 90 rearrangement breakpoints in 41 BACs with some BACs containing multiple breakpoints (Table 3 and Table S2 in Additional data file 3). Breakpoints in six clones could not be identified due to repetitive elements and/or genome assembly problems [See Additional data file 1]. The sequencing of these 41 clones confirmed the genomic locations of the BES determined by ESP and identified translocation breakpoints in primary tumors of the breast, brain, ovary, and a metastatic prostate tumor. In the breast cancer cell line MCF7, all clones with multiple breakpoints mapped to a highly rearranged amplicon of colocalized DNA from chromosomes 1, 3, 17, and 20, consistent with an earlier report [7] demonstrating that up to 11 breakpoints can be present in a single 150-kb clone.

Of the 90 breakpoints identified in these 41 BACs, 63 were sequenced, and the remaining 27 were localized to 3-kb subclones. Since gross genomic rearrangements result from aberrant double strand break (DSB) repair, we analyzed the rearrangement breakpoints for signatures of the two major DBS repair mechanisms: non-allelic homologous recombination and non-homologous end joining (NHEJ). We analyzed the repeat content and structure of the 63 breakpoint junctions, 53 of which were non-redundant [See Table

S3 in Additional data file 3]. These 53 non-redundant junctions encompass 31 translocations, 12 deletions and 10 inversions. Two junctions (representing two translocations) contain Alu elements spanning the breakpoints and are consistent with DSB repair by Alu-mediated non-allelic homologous recombination. All of the remaining junctions (51/53, 96%) are consistent with NHEJ repair and either span microhomology regions ranging in size from 1 to 33 bp (45/51) or lack any homology (6/51) between the two regions involved in a particular rearrangement. We find insertions at the junction site ranging from 1 to 31 bp in 7/51 NHEJ events. Twenty of the 106 breakpoint sites deduced from the non-redundant junction analyses are located within regions of known structural variation.

Of the 90 breakpoints, 72 are predicted to alter gene structure resulting in either gene fusions or fusions of gene fragments to intergenic regions. This high proportion reflects a nonrandom selection of clones for sequencing, with priority given to clones likely to encode fusion genes [12]. Of the remaining 18 breakpoints, 3 indicate deletions of multiple genes. For example a breakpoint on chromosome 17 indicates a deletion of five genes (*EFCAB3*, *METTL2A*, *TLK2*, *MRC2*, and *RNF190*). An additional 7 breakpoints are located within genes and may result in intragenic rearrangements (e.g. the *DEPDC6* gene on chromosome 8). The remaining 8 breakpoints are either rearrangements involving intergenic regions or microrearrangements within introns.

Breakpoint Heterogeneity

BAC clones in amplicons such as those on chromosomes 1, 3, 17, and 20 in MCF7 are highly over-represented and consequently form large BES clusters of invalid pairs. Sequencing of a few of these clones [7] revealed that they often span multiple breakpoints. We assessed whether all clones in a BES cluster share the same complex internal organization by assaying the presence of sequenced breakpoints by PCR. In total, we examined 23 breakpoints in 41 clones from seven BES clusters. The majority (69/96) of the PCR assays indicated that breakpoints are shared between clones in the same BES cluster. Surprisingly 5 of 7 BES clusters are heterogeneous in breakpoint composition meaning that clones with nearby mapped ends do not necessarily span the same breakpoints [See Table S4 in Additional data file 3]. For example, MCF7 clone 69F1 with one sequenced breakpoint is a member of a cluster with 11 clones, but only 8 of 11 clones contain the 69F1 breakpoint (Figure 2A, B). Another clone, 37E22, was previously shown to contain four breakpoints [7]. Of the three clones in the BES cluster with 37E22, two clones contain all four breakpoints, while one contained only one of the breakpoints (Figure 2 C). In all cases, PCR validated the end locations of all negative clones confirming the presence of alternative breakpoints in these clones. While the mapped end sequences of the clones in these heterogeneous clusters confirmed that they fuse similar genomic loci, we hypothesize that similar rearrangements occurred in multiple copies of these loci, either due to earlier duplications in MCF7 or genomic heterogeneity in different cells in the MCF7 population. While such variability in breakpoint location, or breakpoint wandering, is observed in fusion genes shared across multiple patients (e.g. the *BCR-ABL* gene in leukemia [13] and there are numerous reports of genomic heterogeneity in cell lines [14, 15], this is the first time that it has been observed on a microgenomic scale within a single sample.

Rearrangement validation

We validated a subset of breakpoints detected in the BT474 and SKBR3 breast cancer cell lines using dual-color FISH. Normal BAC clones were selected that flank the predicted breakpoints in the reference human genome, and FISH was performed to metaphase spreads from the cell lines. Four BT474 and two SKBR3 breakpoints were confirmed using dual color FISH (Figure 3). In addition DNA fingerprinting was employed [16-20] on a subset of clones from the MCF7, brain and breast (B421) BAC libraries. Excellent correlation between BES mapping and fingerprint mapping was observed: fingerprint analysis confirmed the absence of the rearrangements in 250 of 261 (96%) BAC clones predicted not to span rearrangement breakpoints and confirmed the presence of breakpoints in 154 of 226 (68%) clones predicted to span genomic breakpoints by ESP [21].

Identification and analysis of recurrent breakpoints

We clustered BES pairs from all ESP datasets together and identified 62 *recurrent clusters* that contain BES pairs from multiple samples whose mapped ends are close. Recurrent clusters may be caused by recurrent somatic mutations, structural polymorphisms [22], mapping problems or assembly errors in the reference genome. Most recurrent clusters (60/62) fall into two classes: (i) mapping to pericentromeric/subtelomeric regions (9) or (ii) *micro-rearrangements* (56), defined here as rearrangements with breakpoints less than 2 Mb apart. Five clusters fall into both classes. For the micro-rearrangements, 21/56 (38%) overlap known structural variants [23] [See Table S5 in Additional data file 3], nearly a three-fold enrichment over the 15% of non-recurrent clusters corresponding to known structural variants. The remaining 35 clusters may detect novel structural variants or cancer-specific rearrangements. For example, a pericentric inversion on chromosome 11 was identified in two breast tumors and all three breast cell lines [See Table S6 in Additional data file 1]. Other examples include an 820-kb deletion in 17q23.3 in MCF7 and BT474 that contains the *TRIM37*, *GDPD1*, *YPEL2*, *DHX40*, and *CLTC* genes and a 4 Mb deletion of gene-rich region in 10q11.22-10q11.23 in BT474 and a primary breast tumor (CHORI514) [See Table S6 in Additional data file 1 and Figure S3 in Additional data file 2].

The largest number of BES clusters is found in the ESP datasets from the breast cancer cell lines BT474, MCF7, and SKBR3. ESP identifies known amplicons, deletions, and translocations present in these cell lines [24-26]. We searched for genomic loci that contain a rearrangement breakpoint in at least two of these three cell lines. To minimize the possibility of experimental errors, we first restricted consideration to rearrangement breakpoints identified by a BES cluster in each cell line. We identified six examples of such recurrent rearrangement loci. Four loci shared between MCF7 and BT474 map to the 20q13.2-20q13.3 amplicon and have ends clustered within 2 Mb (Figure 4 A,B). It might be significant that the breakpoints in MCF7 occur in and/or truncate BCAS1, possibly explaining its total lack of expression in MCF7 despite being amplified [27]. In contrast, BCAS1 is highly amplified and expressed in BT474 [27], and the breakpoints map immediately distal to BCAS1 (Figure 4A). In addition, the regular spacing of breakpoints in this locus is suggestive of breakage/fusion/bridge (B/F/B) cycles [7]. Two additional loci are common to BT474 and SKBR3. One locus includes breakpoints that cluster within ~ 500 kb of the ERBB2 gene that is amplified and over-expressed in these

cell lines [26]. In SKBR3, these breaks colocalize the *ERRB2* locus with an amplified region from chromosome 8 (Figure 4C). In the last example, breakpoints in BT474 and SKBR3 are predicted to disrupt the ubiquitin protein ligase gene *ITCH* at 20q11.2. When considering rearrangement breakpoints defined by all invalid pairs, rather than only BES clusters, we identified 88 recurrent rearrangement loci across the three breast cancer cell lines [See Table S7 in Additional data file 3].

Identification of fusion transcripts

Comparison of breakpoints revealed by ESP and putative fusion transcripts identified in public EST databases provides evidence for expressed gene fusions. In one case, ESP identified two BAC clones spanning an apparent 1q21.1;16q22.2 translocation in MCF7 and a primary breast tumor, (MCF7_1-30J11 and 2B421_023-O08, respectively). Both clones were sequenced, and found to span identical breakpoints [See Table S8 in Additional data file 3]. An EST clone DR000174 was identified in Genbank that co-localizes with the sequenced breakpoint in BAC clones. This EST fuses a part of exon 6 with an adjoining intron of the *HYDIN* gene to an anonymous gene represented by a cluster of spliced EST sequences. RT-PCR provided clear evidence that the fusion transcript is expressed in 16 of 21 breast cancer cell lines (Figure 5A and Additional data file 1), normal cultured human breast epithelial cells, and a wide range of normal human tissues. Recently, a 360-kb segmental duplication containing the *HYDIN* locus was identified on chromosome 1q21.1 [28]. This duplication event created the *HYDIN* fusion gene and explains the observed apparent 1q21.1;16q22.2 translocation. To our knowledge this is the first example of a segmental duplication resulting in an expressed fusion gene.

In a second example, a putative fusion transcript (GenBank accession CN272097) and the breakpoint in MCF7 clone 1-97B19 identify a complex rearrangement fusing the SLC12A2 gene and EST AK090949 on chromosome 5. RT-PCR provided evidence for expression of the fused transcript in 5 of 21 breast cancer cell lines and in higher passage, but not lower passage, human mammary epithelial cells (Figure 5B). In addition, RT-PCR provided clear evidence of alternative splicing of this transcript. Interestingly, we do not detect expression of this fusion transcript in MCF7 possibly due to differences between the location of this breakpoint in MCF7 and the EST. If this fusion is the result of a somatic mutation in breast tumors and not a structural polymorphism, it will represent the first recurrent fusion transcript reported in breast cancer. Additional studies aimed at analysis of the presence of this transcript in clinical specimens are underway. Thus, paired-end sequencing approaches are useful for the elucidation of genome and transcriptome remodeling in phylogenetics and cancer.

SNP Analysis

The availability of ~89 Mb of sequence from 97,680 mapped BES made it possible to identify single nucleotide polymorphisms and candidate somatic mutations. Approximately 62.5% (61,013) of the mapped BES contained at least one mismatch in the alignment between the BES and the reference genome. From these mismatches, we identified 115,444 candidate SNPs defined as a single base mismatch flanked on both sides by at least one matched base. Many of these mismatches are likely sequencing errors to be expected when examining raw end sequences. Thus, we applied the following filtering criteria to discard low confidence SNPs: the PHRED score [29] of the

SNP, the mean PHRED score of the five bases centered on the SNP, and the mean PHRED score of the entire BES containing the SNP all must exceed 30. Approximately 58% of the candidates SNPs were removed by this filtering step, leaving 48,243 SNPs. Of these, 40,659 (84%) are known variants recorded in dbSNP: the probability of this event if our SNP candidates were randomly distributed on the genome, as would be the case if they were largely caused by sequencing errors, is vanishingly small. Thus, our stringent filtering criteria enriched for true SNPs instead of sequencing errors. 7,584 (~16%) of the valid SNPs are novel [See Table S9 in Additional data file 1], and 77 of them are recorded in more than one BES [See Table S10 in Additional data file 3]. All of the cancer samples show significantly ($P < 10^{-23}$) higher rates of novel SNPs than the normal sample; moreover, the ovarian tumor has a significantly ($P < 10^{-39}$) higher rate of SNPs than the other cancer samples (Figure 6). While some of these novels SNPs are likely to be sequencing errors or rare genetic variants, these cases do not explain the observed biases across samples.

The transition:transversion ratio of these novel candidate SNPs is 1.8, which is lower than the value 1.95 reported for BAC end sequencing of mouse strains [30], comparable to the value 1.85 in coding exons of breast tumors [31], but significantly lower than the value 7.4 in coding exons of colorectal tumors [31]. Moreover, the mutational spectrum of these novel SNPs [See Table S11 in Additional data file 1] varies across the tumor types, and many of these variations are significant ($P < 0.00001$ by χ^2 test). An excess of C:G → T:A transitions over T:A → C:G transitions is observed in all samples except one of the breast tumors, similar to recent reports from exon resequencing studies in tumors [31, 32]. However, the asymmetry in the frequency of these two types of transitions is generally less than reported in these studies. Interestingly, the strongest asymmetry is found in our brain sample, in agreement with [32] who find the greatest asymmetry in gliomas. Examination of the frequency of variation at dinucleotides [See Table S12 in Additional data file 3] reveals an excess of C:G → G:C transversions occurring at TpC/GpA dinucleotides consistent with the report of [32]. The explanation for this bias is not known, but is hypothesized to represent a cancer-specific mutational mechanism or environmental exposure.

Thirty-five of the 7,584 novel SNPs were identified in coding regions [See Table S13 in Additional data file 3]. Of these, 24 are non-synonymous changes that occur in a diverse group of genes including the genes *IRAK1* (possibly mutated in breast tumor B421) and *RPS6KB1* (possibly mutated in BT474), which were previously identified as somatic mutations in breast cancer [33]. Analysis of gene annotations recorded in GO with the DAVID tool [34] that corrects for differences in the sizes of annotated gene families, identified six genes classified as "transition metal ion binding" ($P = 0.07$) including the zinc binding proteins *ZNF217*, *ZNF160*, *ZNF354C*, *ZDHHC4*, and *ANKMY1*. Interestingly, the SNP in *ZDHHC4* occurs in the zinc finger domain as defined in UniProt. Examination of SNPs in amplified regions in MCF7, BT474, and SKBR3 did not suggest any correlation between SNP rate and amplification: some amplicons harbor a high number of sequence variants, while others have relatively few [See Table S14 in Additional data file 3].

We resequenced 17 candidate SNPs found in the breast cancer cell lines [See Table S15 in Additional data file 3] and confirmed 11/17 (64.7%), a success rate is very similar to

the 68% reported in large-scale resequencing of exons [31]. Of the six remaining cases, four were sequencing failures, while two contained double signals in the ABI electrophoregrams at the SNP site, with the reference peak being the dominant one. Thus, it is possible that these SNPs are heterogeneous in the cell lines. Therefore, only 2/17 candidate SNPs (11.8%) were contradicted by resequencing. Since 2 of the 11 validated SNPs, plus two that were not validated were also found in a more recent update of dbSNP (128), we checked all 7584 novel SNPs against dbSNP Build 128 and found that 1698 (22%) were present, providing further evidence that our SNP filtering criteria are enriching for true sequence variants rather than sequencing artifacts.

Discussion

The importance ascribed to different types of genome aberrations in cancer is frequently directly coupled to the technology available to measure them: classic cytogenetics demonstrated the functional significance of translocations in tumors with simple karyotypes, while LOH, CGH and array-CGH studies have led to an explosion of interest in recurrent copy-number aberrations. More recently, targeted [32, 35] and whole genome exon re-sequencing [31] has shown the importance of coding mutations. The Cancer Genome Atlas project [36] promises to drastically increase the number of known coding somatic mutations. However, it is likely that structural rearrangements in tumor genomes are as important to tumor biology and the development of biomarkers and therapeutics as are coding point mutations [37, 38]. We have demonstrated that ESP provides direct access to the structural complexity of tumor genomes by identifying and cloning all classes of structural rearrangements including fusion genes and their transcripts. ESP also proved to be a powerful tool for analysis of structural polymorphism present in the normal human genome [39, 40]. Moreover, identification of the *HYDIN* gene fusion by ESP reveals that duplicon-mediated genome rearrangements can result in expression of structurally novel genes. Using this approach it is also possible to survey the spectrum of mutations and/or SNPs present in a tumor genome in an unbiased fashion.

Many of the recurrent breakpoints that we identified arise from micro-rearrangements of less than 2 Mb (Figure 4). Although some of these rearrangements are likely to be novel structural polymorphisms, micro-rearrangements have also been observed in evolution [41, 42] and in some tumors [43]. Since micro-rearrangements are largely invisible to cytogenetic techniques, the collection of the breakpoints reported in this paper provides an excellent resource for future studies of the mechanisms, prevalence, and consequences of these micro-rearrangements in tumorigenesis.

Sequencing BAC clones identified by ESP was performed to localize and validate ~90 breakpoints in this and a previous study [7]. To our knowledge, this is currently the largest collection of sequenced rearrangement breakpoints in cancer. Importantly, this collection can be easily extended as needed, since ESP created also the largest collection to date of hundreds of sequence-ready breakpoint-spanning BAC clones. Most breakpoint- spanning BAC clones, including all BAC clones sequenced from primary tumors, contain single breakpoints. However, in the three cell lines, 17 clones containing multiple breakpoints were identified and confirmed by PCR. These observations were

supported by DNA fingerprinting (Dr. Marco Marra; personal communication and [21]). The observed differences between the primary tumors and cell lines may be due to genomic heterogeneity (and consequently lower sequence coverage) of tumor samples, differences in tumor type and/or stage, or intrinsic differences in genomic organization between cell lines and primary tumors. It will be informative to perform ESP on primary breast tumors with copy-number profiles very similar to those of the cell lines studied here [10, 11] and to establish the degree of the structural similarity of the samples with similar copy-number and expression profiles.

Our analyses of breakpoint junction sequences revealed that the overwhelming majority of identified rearrangements (96%) are consistent with aberrant NHEJ repair. This observation is consistent with the previously reported predominant role of non-homologous recombination in generation of pathologic translocations [44] and in frequent rearrangements at chromosomal ends [45]. While there are reports of associations between locations of cancer breakpoints and evolutionary breakpoints [46], ESP data did not reveal a significant association in our samples (data not shown).

We used sequenced breakpoints to refine the mapping of amplicon structures in MCF7 using PCR in seven independent BES clusters. This process identified breakpoint heterogeneity in five clusters (Figure 2 and Figure S3 in Additional data file 2). One explanation for this phenomenon is variability in the location of breakpoints in multiple fusions of the same loci, analogous to the variability of breakpoints in fusion genes in hematopoietic malignancies. Alternatively, the heterogeneity might reflect early events present in a minority of cells in the population. To our knowledge, this is the first example of structural heterogeneity observed on a molecular level in tumor genomes.

Analysis of SNPs in BAC end sequences identified elevated rates of SNPs in each tumor sample compared to the normal sample, with the ovarian tumor exhibiting a rate significantly above the other samples. Although the ability to distinguish somatic mutations from sequencing errors or germline mutations is limited in the present study, there is no reason to suspect that these confounding factors vary enough between samples to explain the observed differences. The mutational spectra of SNPs in these samples share some features with those from exon resequencing studies [31, 32], but there are also many differences. These differences might be due to different mutational biases in coding regions, but further study is needed to support this hypothesis. Given that the BES arise from a genome-wide survey, it is not surprising that we identify few candidate mutations in coding regions. However, it is intriguing that even the relatively small numbers of putative mutations are enriched for zinc finger genes, including the known breast cancer oncogene *ZNF217* [27, 47, 48].

Using ESP it is possible to reconstruct tumor genome structure and evolution [4-7]. ESP data from the three breast cancer cell lines identify clones that fuse noncontiguous amplified loci, possibly suggesting functional coupling of co-amplified genes. The discovery of recurrent breakpoints and regularly spaced breakpoints in the cell-line data could be a molecular signature of breakage/fusion/bridge (B/F/B) cycles [7]. In some cases, ESP data suggest a specific temporal progression where amplification follows translocations or deletions. For example, a cluster of 19 clones span a 17;20 translocation in MCF7. This coverage is highly unlikely ($P < 10^{-20}$) for a non-amplified locus and PCR mapping confirmed identical breakpoints in these clones. The most parsimonious

explanation is that the translocation preceded the amplification. In a second example, a cluster of six BT474 clones spans a deletion. Once again the simplest explanation is that the deletion preceded amplification of the surrounding locus, since a cluster of size six clones is highly unlikely ($P \approx 10^{-5}$) in a non-amplified locus. Interestingly, this deletion may truncate the *THRA1* gene as reported in [25] and fuse it to the *SCAP1* gene. Amplification of a breakpoint might occur because the fused genomic region encodes a fusion gene that confers a selective growth advantage. Alternatively, amplification might be a random byproduct of genomic instability near the rearrangement breakpoint. Regardless, the breakpoint information is valuable for determining the temporal evolution of tumor genome organization.

The identification of *TMPRSS2* translocations in ~ 50% of prostate tumors [3] underscores the significance of structural rearrangements in solid tumors. While our prostate sample does not contain the *TMPRSS2* translocation (Mark Rubin, personal communication), ESP mapping and breakpoint sequencing provide numerous examples of possible gene fusions, including the previously published *BCAS4/3* fusion in MCF7. Moreover, integration of public EST data with ESP data demonstrates that this approach can identify fusion transcripts *en masse*. We identified a fusion transcript that results from an evolutionarily recent rearrangement of the normal genome and obtained evidence for the first recurrent fusion transcript in breast cancer. In this study the clonal coverage of tumor genomes ranged from only .15 to .7-fold redundancy. It is probable that many additional gene fusions will be identified upon deeper paired end analysis of both normal and tumor genomes and transcriptomes.

The extension of ESP to multiple tumor types demonstrates that its application is not restricted to specific tumor types and that ESP functions well even with small tumor specimens. This is important because advances in diagnostics have resulted in a reduction in the average volume of many surgically excised tumors. For example, the average size of breast tumors excised before 1985 was 25 mm, while after 1985 it decreased to 21 mm [49], a 1.6 fold decrease in the volume of excised breast tumors. Moreover, tumor heterogeneity and normal cell admixture necessitates dissection further reducing subsequent yields of tumor cell DNA. Finally, clinically annotated tumor specimens are an extremely valuable resource and should be used as sparingly as possible. Therefore, it is significant that we were able to construct a tumor BAC library from less than 20 mg of a frozen and partially necrotic tumor (B421). DNA yields from the tumors suggest that libraries comprised of 200,000-400,000 clones are possible, meaning that the genomes of these tumors can be immortalized and made widely available. This study demonstrates the utility of ESP for whole genome screening of SNPs/mutations. The immortalization of the tumor genome in a clone library is important, since some studies report underestimation of the mutation load because of heterogeneity in tumors [50], and overcoming this problem will require either development of the novel software, or implementation of the novel sequencing technologies allowing analysis of single DNA molecules [51]. Since clone libraries can be duplicated and their DNA pooled, it becomes feasible to perform large exon resequencing projects on small tumors such as those of the breast and prostate. In addition, since BAC clones contain DNA from a single tumor cell, identification of rare SNPs/mutations in heterogeneous tumors is theoretically possible in

a manner analogous to the identification of breakpoint heterogeneity in tumor amplicons reported here. Finally, the ability to rapidly identify sequence variants in DNA pools and to then recover the physical clone means that studies aimed at determining the biological relevance of the variants are possible using established *in vivo* and *in vitro* systems.

ESP is less impeded by tumor heterogeneity or contamination by normal cells than is aCGH, because each end-sequenced clone originates from a single DNA molecule from a single cell. Deep sequencing of many clones allows one to overcome normal tissue admixture and enables direct measurements of heterogeneity and detection of rare events. Eventually it will be possible to apply techniques from metagenomics [52] to study the heterogeneous pool of cells present in early stage tumors with the goal of identifying the earliest informative biomarkers and therapeutic targets. At present, the relatively high cost of ESP limits its application to a small number of tumors, but advances in massively parallel sequencing technologies capable of paired-end sequencing (reviewed in [9]) will permit large-scale ESP studies at a fraction of the current cost. However, much of the cost savings realized by the current crop of next-generation sequencing technologies result from skipping the immortalization of the tumor genome as a clone library. Such cloning enables further sequencing of breakpoints and evaluation of their functional significance via *in vitro* and *in vivo* assays [7]. Combining ESP with such assays will enable tumor progression studies aimed at identification of events linked to initiation, progression, and metastasis. Thus, while the selection of a particular implementation of ESP will be driven by the cost/benefit analysis for the specific goals of the project, paired end sequencing approaches promise to revolutionize our understanding of the complex organization of the genomes of solid tumors.

Materials and methods

BAC Library Construction

Breast cancer cell lines were obtained from UCSF cell culture facility. Clinical tumor specimens were obtained from Bay Area Breast Oncology Program (breast tumors), rapid autopsy program at University of Michigan [53], and the University of Texas M.D. Anderson Cancer Center SPORE in ovarian cancer (ovarian).

Library preparation was carried out as described previously [7] (see detailed protocol at [54]). Briefly, fresh frozen tissue (0.1 to 0.15 g) was slowly thawed on ice, ground and resuspended in 0.6 mL of 1X PBS (pH 7.0). The suspension was pre-warmed to 42°C in water bath and mixed with an equal amount of a warm 1.5% solution of low melting-point agarose. The partial restriction was carried out for 1 hour on ice, followed with incubation for 10 min at 37°C and stopped by addition of 0.1 volume of 0.5 M EDTA. Additional processing associated with isolation of high molecular weight DNA, construction of BAC libraries and end-sequencing of BAC clones was carried out as previously reported [7].

ESP Data Analysis

We employed a two-step procedure that involved first mapping the BAC end sequence (BES) data onto the human genome sequence (NCBI Build 35, May 2004), and then filtering the mapping results. The mapping step is accomplished using BLAT [55]. A location is assigned if at least 50 bp of a BES aligned to the reference genome sequence with at least 97% identity. If the BES hit multiple locations in the genome, the position of the longest hit with highest identity was chosen and the BES was designated as being "ambiguously mapped" and excluded from further analysis. Finally, BES mapping to known segmental duplications, as defined by the SegmentalDups track of the UCSC Genome Browser were removed. Only clones corresponding to unique BES pairs were retained. BES mappings are available as a custom track for the UCSC Genome Browser at [56].

BES pairs with BES mapping to the same chromosome and having opposite convergent orientations (i.e., a pair of the form ([chrom1, loc1, strand1], [chrom2, loc2, strand2]) with chrom1 = chrom2, loc1 < loc2, strand1 = "+", and strand2 = "-") were identified. The distribution of distances between mapped ends (loc2 – loc1) was used to define the length distribution of the BAC libraries. BES pairs with ends on the same chromosome and having convergent orientations on opposite strands and distances in the 99.5% quantile of this distribution were classified as *valid*. Other BES pairs were classified as *invalid* and thus candidate rearrangements in the tumor. Note that the distance criterion was very permissive and might misclassify clones harboring small indels as valid. Overlapping valid pairs were combined into "contigs", while invalid pairs were clustered into sets according to whether their locations were close enough to be explained by a single rearrangement event [4-7]. Invalid pairs (or clusters) were classified as potential indels, inversions, or translocations according to the location and orientation of their ends [See Table S1 in Additional data file 1].

Custom software was used to visualize the mapping results as described in [6]. A plot of BES density generated a copy-number profile for the entire tumor genome, as the overall number of BES per given genomic interval is roughly proportional to copy number.

Known Structural Variants

Locations of previously reported structural variants were downloaded from the Database of Genomic Variants [23, 57]. Clusters of invalid BES pairs were labeled as "explained" by the known structural variant if the locations of the variant overlapped the locations of an end sequence pair in the cluster, and the type of variant was consistent with the orientations of the mapped end sequences in the clusters. That is, pairs with convergent orientation are consistent with insertions and deletions (i.e. copy number variants), while pairs with the same orientation are consistent with inversions. We did not require precise overlap between the breakpoints of the invalid BES pairs and the breakpoints of the structural variants because both types of breakpoints were only approximately known. Note that multiple structural variants might "explain" a cluster because the structural variants in the database were merged from different experimental sources and have some redundancy [58].

BAC Sequencing

BAC DNA was purified from 250 ml overnight culture using the Qiagen columns (Qiagen). Approximately 2 μg of BAC DNA was mechanically sheared using the HydroShear (GeneMachine Inc.), end-repaired with the Klenow enzyme and T4 DNA polymerase, size-selected for 3±0.5 kb fragments on agarose gels, and cloned into a pUC19 vector. Individually picked subclones were grown on 96-well plates overnight in LB plus 200 μg/ml ampicilin and 10% glycerol. Plasmid DNA was prepared from the arrayed cells using the TempliPhi kit (GE/Amersham) according to the manufacturer's protocol. 3 kb subclones were end-sequenced using BigDye terminators (Applied Biosystems) and capillary sequencers. Quality of the sequence reads were determined by Phred score [29], and only sequences greater than Q20 were included in the analysis.

Analysis of rearrangements breakpoint junctions

Breakpoint junction sequences were aligned to the Human Genome Assembly (NCBI Build 35, May 2004) using BLAT [55], and the alignments were analyzed for the precise position of the breakpoint and presence of microhomologies. Breakpoint sequences were also analyzed for their repeat content using the RepeatMasker program and for their overlap with known copy number polymorphic regions using the Structural Variation track of the Genome Browser. The mechanism of each rearrangement was deduced from the alignment of the breakpoint junction sequence to the native sequences of the two regions participating in the rearrangement, and the number of total DSBs calculated as previously described [45].

SNP Analysis

Out of the ~70,000 clones sequenced for this and previous studies, we selected the 97,860 BES that mapped to unique loci on the hg17 reference genome with a minimum BLAT identity score of 97%. The mean PHRED score [29] of these BES is 51. 61,013 of the selected BES contained at least one mismatch. Runs of multiple contiguous mismatches and indels were not considered when defining a SNP. We identified 115,444 candidate SNPs, which we defined as a single base mismatch flanked on both sides by at least one matched base. 67,201 (58.21%) of these candidate SNPs were attributed to possible sequencing errors, because the PHRED score of the SNP, or the mean PHRED score of the five bases centered on the SNP, or the mean PHRED score of the entire BES was below 30. Candidate SNPs were not considered tumor-specific if their location and nucleotide change matched a known SNP in dbSNP Build 124. Coding SNPs were identified as those than lie in exons annotated from the "Known Genes" track of the UCSC Genome Browser. The observed rates of SNPs of each type of nucleotide substitution were compared across different samples using the chi-square test. Enrichment of GO terms for the genes containing candidate SNPs was computed with the DAVID tool [34], which computes P-values for enrichment correcting for the size of the gene sets in each term. We used the LiftOver tool from the UCSC Genome Browser [59] to identify the locations of each novel SNP in the latest build (Build36) of the human reference genome and examined whether these SNPs were present in dbSNP Build 128

using the snp128 table. The validation of candidate SNPs/mutations was performed by direct genomic sequencing of the DNA amplified from the cell line used for ESP.

Reverse-Transcript PCR

RT-PCR experiments were carried out as described in [60]. Primer sequences and conditions are presented in table below. We employed a nested PCR strategy to increase specificity and sensitivity of our assay. All PCR reactions were carried out in 25 μl reaction volumes using following program: initial denaturation of DNA – 4 min at 94°C, 30 to 35 cycles of 15 sec at 94°C, 30 sec at 60°C, 45 sec at 72°C. We have used ~100 ng of cDNA for the first reaction with outer primers, and 1 μl of the resulting PCR reaction for the second round using inner primers. Following primers were used: DR00074: AGGAAAAGGCCTTGAAGCTC and TGCTGTATTTGACAGGACAAGTG (outer primers); GAGGACATGCTCCTACCTGTG and TGCTGTATTTGACAGGACAAGTG (inner). For CN272097 we used CCAACGTGAGCTTCCAGAAC and ACAGAAACGCCTCTTCTCATTTAG (outer); TATTATGATACCCACACCAACACC and CTCCTGTTCGTGTCAGCAATAC (inner). The specificity of PCR reactions were validated by sequencing at UCSF Genome Analysis Core.

Spectral karyotyping (SKY) and FISH analysis:

Cells lines were shipped to HPN. When cell lines reached 70% confluence, cells were treated with colcemid (Roche, Indianapolis, IN) for 1 hour to arrest the cells in mitosis. Metaphase chromosome suspensions were prepared first by treating cells with a hypotonic solution (0.075M KCl), next, the cells were fixed using methanol: acetic acid (3:1, vol/vol) and dropped onto slides in a humidity controlled chamber. The slides were aged at 37°C for approximately one week. Chromosome preparations were hybridized with either FISH probes or SKY probes for 72 hours. The protocols for preparation of FISH/SKY probes, slide pre-treatment, slide denaturation, detection, and imaging have been described previously and are available at [61]. Ten to 15 metaphase spreads were analyzed per sample and scored for the following: chromosome number (ploidy), numerical aberrations, and structural aberrations. Spectrum-based classification and analysis of the fluorescent images (SKY) was achieved using SkyView^{TM} software (Applied Spectral Imaging, Carlsbad, CA). The karyotypes of every metaphase spread from all groups were characterized using the human chromosome nomenclature rules described in ISCN, 2005.

Abbreviations

ESP, end sequencing profiling; FISH, fluorescence *in situ* hybridization; SNP, single nucleotide polymorphism; BAC, bacterial artificial chromosome; BES, BAC end sequence; SKY, spectral karyotyping; EST, expressed sequence tag; aCGH, array comparative genomic hybridization.

Authors' contributions

BJR analyzed the data including identification and analysis of sequence variants, clustering of the identified breakpoints, and comparison of ESP and aCGH data. SV and CC developed the ESP methodology and BES mapping algorithms, analyzed the data and

coordinated the clinical samples, sequencing, and experimental validation of ESP results. PY and CW integrated ESP and public EST data, and identified fusion transcripts. EL and BT performed analysis of sequenced breakpoints and contributed to paper writing. FW selected and managed the breast clinical specimens and developed the FISH methods of breakpoint validation. JC, KJP, GBM managed and selected the brain, prostate, ovary tumor samples, respectively. PP, KB, YK, G-QH and SS performed experimental validation. AB, RB, and SJA performed analysis of fusion genes and sequence variants. JWG and J-FC sequenced BAC clones. QT, PdJ, and MN constructed BAC libraries. HP-N and TR performed FISH validation and experimental validation of ESP breakpoints. BJR, SV, and CC wrote the paper. All authors read and approved the final manuscript.

Additional data files

The following additional data are available with the online version of this paper. Additional data file 1 contains supplemental text and tables, including a description of all supplemental tables. Additional data file 2 contains three supplemental figures. Additional data file 3 contains supplemental tables.

Acknowledgements

The work in the C.C. laboratory was supported by the grants from the NIH/NCI (R33 CA103068), the Breast Cancer Research Program (8WB-0054), the Susan G. Komen for the Cure Foundation (BCTR0601011), the Prostate Cancer Foundation, the Bay Area Breast Cancer Spore (CA5807), and a developmental research program award from UCSF brain tumor SPORE. B.J.R. is supported by a Career Award at the Scientific Interface (CASI) from the Burroughs Wellcome Fund, and a fellowship from the Alfred P. Sloan Foundation. The work in the B.J.T. laboratory was supported by NIH RO1 GM057070. S.J.A is supported by a William R. Hewlett Stanford Graduate Fellowship and a National Science Foundation Fellowship. R.P.B. is supported by a Ruth L. Kirschstein National Research Service Award – NIH Bioinformatics Training Grant No. GM00806-06. K.J.P is supported by SPORE P50 CA69568. J.W.G is supported by the Director, Office of Science, Office of Basic Energy Sciences, of the U.S. Department of Energy under Contract No. DE-AC02-05CH11231, by the USAMRMC BC 061995, and by the National Institutes of Health, National Cancer Institute grants P50 CA 58207, the P50 CA 83639 the P30 CA 82103, the U54 CA 112970, the U24 CA 126477 and the P01 CA 64602, the NHGRI U24 CA 126551 and by the SmithKline Beecham Corporation grant to J.W.G. The work in the J.-F.C. laboratory was supported by National Heart, Lung, and Blood Institute, Programs for Genomic Applications Grant No. UO1HL66728. The work in the T.R. laboratory was supported in part by the Intramural Research Program of the NIH, National Cancer Institute, Center for Cancer Research.

References

1. **Pinkel D, Albertson DG: Array comparative genomic hybridization and its applications in cancer. *Nat Genet* 2005, 37 Suppl:S11-17.**

2. **Nahta R, Esteva FJ: HER2 therapy: molecular mechanisms of trastuzumab resistance. *Breast Cancer Res* 2006, 8:215.**

3. **Tomlins SA, Rhodes DR, Perner S, Dhanasekaran SM, Mehra R, Sun XW, Varambally S, Cao X, Tchinda J, Kuefer R, et al: Recurrent fusion of TMPRSS2 and ETS transcription factor genes in prostate cancer. *Science* 2005, 310:644-648.**

4. **Raphael BJ, Volik S, Collins C, Pevzner PA: Reconstructing tumor genome architectures. *Bioinformatics* 2003, 19 Suppl 2:II162-II171.**

5. **Raphael BJ, Pevzner PA: Reconstructing tumor amplisomes. *Bioinformatics* 2004, 20 Suppl 1:I265-I273.**

6. **Volik S, Zhao S, Chin K, Brebner JH, Herndon DR, Tao Q, Kowbel D, Huang G, Lapuk A, Kuo WL, et al: End-sequence profiling: sequence-based analysis of aberrant genomes. *Proc Natl Acad Sci U S A* 2003, 100:7696-7701.**

7. **Volik S, Raphael BJ, Huang G, Stratton MR, Bignel G, Murnane J, Brebner JH, Bajsarowicz K, Paris PL, Tao Q, et al: Decoding the fine-scale structure of a breast cancer genome and transcriptome. *Genome Res* 2006, 16:394-404.**

8. **Bignell GR, Santarius T, Pole JC, Butler AP, Perry J, Pleasance E, Greenman C, Menzies A, Taylor S, Edkins S, et al: Architectures of somatic genomic rearrangement in human cancer amplicons at sequence-level resolution. *Genome Res* 2007, 17:1296-1303.**

9. **Bentley DR: Whole-genome re-sequencing. *Curr Opin Genet Dev* 2006, 16:545-552.**

10. **Chin K, DeVries S, Fridlyand J, Spellman PT, Roydasgupta R, Kuo WL, Lapuk A, Neve RM, Qian Z, Ryder T, et al: Genomic and transcriptional aberrations linked to breast cancer pathophysiologies. *Cancer Cell* 2006, 10:529-541.**

11. **Neve RM, Chin K, Fridlyand J, Yeh J, Baehner FL, Fevr T, Clark L, Bayani N, Coppe J-P, Tong F, et al: A collection of breast cancer cell lines for the study of functionally distinct cancer subtypes. *Cancer Cell* 2006, 10:515-527.**

12. **Bashir A, Volik S, Collins C, Bafna V, Raphael BJ: Evaluation of Paired-end Sequencing Strategies for Detection of Genome Rearrangements in Cancer. *PLOS Computational Biology* 2008, In Press.**

13. **Westbrook CA, Rubin CM, Carrino JJ, Le Beau MM, Bernards A, Rowley JD: Long-range mapping of the Philadelphia chromosome by pulsed-field gel electrophoresis.** ***Blood*** **1988, 71:697-702.**

14. **Klein A, Jung V, Zang KD, Henn W, Montenarh M, Kartarius S, Steudel WI, Urbschat S: Detailed chromosomal characterization of the breast cancer cell line MCF7 with special focus on the expression of the serine-threonine kinase 15.** ***Oncol Rep*** **2005, 14:23-31.**

15. **Nugoli M, Chuchana P, Vendrell J, Orsetti B, Ursule L, Nguyen C, Birnbaum D, Douzery EJ, Cohen P, Theillet C: Genetic variability in MCF-7 sublines: evidence of rapid genomic and RNA expression profile modifications.** ***BMC Cancer*** **2003, 3:13.**

16. **Flibotte S, Chiu R, Fjell C, Krzywinski M, Schein JE, Shin H, Marra MA: Automated ordering of fingerprinted clones.** ***Bioinformatics*** **2004, 20:1264-1271.**

17. **Fuhrmann DR, Krzywinski MI, Chiu R, Saeedi P, Schein JE, Bosdet IE, Chinwalla A, Hillier LW, Waterston RH, McPherson JD, et al: Software for automated analysis of DNA fingerprinting gels.** ***Genome Res*** **2003, 13:940-953.**

18. **Krzywinski M, Bosdet I, Smailus D, Chiu R, Mathewson C, Wye N, Barber S, Brown-John M, Chan S, Chand S, et al: A set of BAC clones spanning the human genome.** ***Nucleic Acids Res*** **2004, 32:3651-3660.**

19. **Krzywinski M, Volik S, Bosdet I, Brebner J, Mathewson C, Wye N, Brown-John M, Chiu R, Cloutier A, Featherstone R, et al: Application of Multiple Digest BAC Fingerprints to Detect Chromosomal Aberrations in Cancer. In** ***Biology of Genomes*****;** ***2004; Cold Spring Harbor Laboratory, NY*****. 2004**

20. **Ness SR, Terpstra W, Krzywinski M, Marra MA, Jones SJ: Assembly of fingerprint contigs: parallelized FPC.** ***Bioinformatics*** **2002, 18:484-485.**

21. **Krzywinski M, Bosdet I, Mathewson C, Wye N, Brebner J, Chiu R, Corbett R, Field M, Lee D, Pugh T, et al: A BAC clone fingerprinting approach to the detection of human genome rearrangements.** ***Genome Biol*** **2007, 8:R224.**

22. **Feuk L, Carson AR, Scherer SW: Structural variation in the human genome.** ***Nat Rev Genet*** **2006, 7:85-97.**

23. **Iafrate AJ, Feuk L, Rivera MN, Listewnik ML, Donahoe PK, Qi Y, Scherer SW, Lee C: Detection of large-scale variation in the human genome.** ***Nat Genet*** **2004, 36:949-951.**

24. **Barlund M, Monni O, Weaver JD, Kauraniemi P, Sauter G, Heiskanen M, Kallioniemi OP, Kallioniemi A: Cloning of BCAS3 (17q23) and BCAS4**

(20q13) genes that undergo amplification, overexpression, and fusion in breast cancer. ***Genes Chromosomes Cancer*** **2002, 35:311-317.**

25. Futreal PA, Cochran C, Marks JR, Iglehart JD, Zimmerman W, Barrett JC, Wiseman RW: Mutation analysis of the THRA1 gene in breast cancer: deletion/fusion of the gene to a novel sequence on 17q in the BT474 cell line. ***Cancer Res*** **1994, 54:1791-1794.**

26. Pollack JR, Sorlie T, Perou CM, Rees CA, Jeffrey SS, Lonning PE, Tibshirani R, Botstein D, Borresen-Dale AL, Brown PO: Microarray analysis reveals a major direct role of DNA copy number alteration in the transcriptional program of human breast tumors. ***Proc Natl Acad Sci U S A*** **2002, 99:12963-12968.**

27. Collins C, Rommens JM, Kowbel D, Godfrey T, Tanner M, Hwang SI, Polikoff D, Nonet G, Cochran J, Myambo K, et al: Positional cloning of ZNF217 and NABC1: genes amplified at 20q13.2 and overexpressed in breast carcinoma. ***Proc Natl Acad Sci U S A*** **1998, 95:8703-8708.**

28. Doggett NA, Xie G, Meincke LJ, Sutherland RD, Mundt MO, Berbari NS, Davy BE, Robinson ML, Rudd MK, Weber JL, et al: A 360-kb interchromosomal duplication of the human HYDIN locus. ***Genomics*** **2006, 88:762-771.**

29. Ewing B, Hillier L, Wendl MC, Green P: Base-calling of automated sequencer traces using phred. I. Accuracy assessment. ***Genome Res*** **1998, 8:175-185.**

30. Abe K, Noguchi H, Tagawa K, Yuzuriha M, Toyoda A, Kojima T, Ezawa K, Saitou N, Hattori M, Sakaki Y, et al: Contribution of Asian mouse subspecies Mus musculus molossinus to genomic constitution of strain C57BL/6J, as defined by BAC-end sequence-SNP analysis. ***Genome Res*** **2004, 14:2439-2447.**

31. Sjoblom T, Jones S, Wood LD, Parsons DW, Lin J, Barber T, Mandelker D, Leary RJ, Ptak J, Silliman N, et al: The Consensus Coding Sequences of Human Breast and Colorectal Cancers. ***Science*** **2006.**

32. Greenman C, Stephens P, Smith R, Dalgliesh GL, Hunter C, Bignell G, Davies H, Teague J, Butler A, Stevens C, et al: Patterns of somatic mutation in human cancer genomes. ***Nature*** **2007, 446:153-158.**

33. Forbes S, Clements J, Dawson E, Bamford S, Webb T, Dogan A, Flanagan A, Teague J, Wooster R, Futreal PA, Stratton MR: Cosmic 2005. ***Br J Cancer*** **2006, 94:318-322.**

34. **Dennis G, Jr., Sherman BT, Hosack DA, Yang J, Gao W, Lane HC, Lempicki RA: DAVID: Database for Annotation, Visualization, and Integrated Discovery. *Genome Biol* 2003, 4:P3.**

35. **Stephens P, Edkins S, Davies H, Greenman C, Cox C, Hunter C, Bignell G, Teague J, Smith R, Stevens C, et al: A screen of the complete protein kinase gene family identifies diverse patterns of somatic mutations in human breast cancer. *Nat Genet* 2005, 37:590-592.**

36. **The Cancer Genome Atlas [http://cancergenome.nih.gov/index.asp]**

37. **Gabor Miklos GL: The human cancer genome project--one more misstep in the war on cancer. *Nat Biotechnol* 2005, 23:535-537.**

38. **Heng HH: Cancer genome sequencing: the challenges ahead. *Bioessays* 2007, 29:783-794.**

39. **Eichler EE, Nickerson DA, Altshuler D, Bowcock AM, Brooks LD, Carter NP, Church DM, Felsenfeld A, Guyer M, Lee C, et al: Completing the map of human genetic variation. *Nature* 2007, 447:161-165.**

40. **Tuzun E, Sharp AJ, Bailey JA, Kaul R, Morrison VA, Pertz LM, Haugen E, Hayden H, Albertson D, Pinkel D, et al: Fine-scale structural variation of the human genome. *Nat Genet* 2005, 37:727-732.**

41. **Bourque G, Pevzner PA, Tesler G: Reconstructing the genomic architecture of ancestral mammals: lessons from human, mouse, and rat genomes. *Genome Res* 2004, 14:507-516.**

42. **Chaisson MJ, Raphael BJ, Pevzner PA: Microinversions in mammalian evolution. *Proc Natl Acad Sci U S A* 2006, 103:19824-19829.**

43. **Graux C, Cools J, Melotte C, Quentmeier H, Ferrando A, Levine R, Vermeesch JR, Stul M, Dutta B, Boeckx N, et al: Fusion of NUP214 to ABL1 on amplified episomes in T-cell acute lymphoblastic leukemia. *Nat Genet* 2004, 36:1084-1089.**

44. **Abeysinghe SS, Chuzhanova N, Krawczak M, Ball EV, Cooper DN: Translocation and gross deletion breakpoints in human inherited disease and cancer I: Nucleotide composition and recombination-associated motifs. *Hum Mutat* 2003, 22:229-244.**

45. **Linardopoulou EV, Williams EM, Fan Y, Friedman C, Young JM, Trask BJ: Human subtelomeres are hot spots of interchromosomal recombination and segmental duplication. *Nature* 2005, 437:94-100.**

46. **Murphy WJ, Larkin DM, Everts-van der Wind A, Bourque G, Tesler G, Auvil L, Beever JE, Chowdhary BP, Galibert F, Gatzke L, et al: Dynamics of**

mammalian chromosome evolution inferred from multispecies comparative maps. *Science* 2005, 309:613-617.

47. Collins C, Volik S, Kowbel D, Ginzinger D, Ylstra B, Cloutier T, Hawkins T, Predki P, Martin C, Wernick M, et al: Comprehensive genome sequence analysis of a breast cancer amplicon. *Genome Res* 2001, 11:1034-1042.

48. Huang G, Krig S, Kowbel D, Xu H, Hyun B, Volik S, Feuerstein B, Mills GB, Stokoe D, Yaswen P, Collins C: ZNF217 suppresses cell death associated with chemotherapy and telomere dysfunction. *Hum Mol Genet* 2005, 14:3219-3225.

49. Sommer HL, Janni, W., Rack, B., Klanner, E., Strobl, B., Rammel, G., Schindlbeck, C., Rjosk, D., Dimpfl, T., Friese, K.: Average tumor size and overall survival of patients with primary diagnosis of breast cancer influenced by a more frequent use of mammography. *Proc Am Soc Clin Oncol* 2003, 22:867.

50. Chanock SJ, Burdett L, Yeager M, Llaca V, Langerod A, Presswalla S, Kaaresen R, Strausberg RL, Gerhard DS, Kristensen V, et al: Somatic sequence alterations in twenty-one genes selected by expression profile analysis of breast carcinomas. *Breast Cancer Res* 2007, 9:R5.

51. Dalgliesh GL, Futreal PA: The continuing search for cancer-causing somatic mutations. *Breast Cancer Res* 2007, 9:101.

52. Venter JC, Remington K, Heidelberg JF, Halpern AL, Rusch D, Eisen JA, Wu D, Paulsen I, Nelson KE, Nelson W, et al: Environmental genome shotgun sequencing of the Sargasso Sea. *Science* 2004, 304:66-74.

53. Rubin MA, Putzi M, Mucci N, Smith DC, Wojno K, Korenchuk S, Pienta KJ: Rapid ("warm") autopsy study for procurement of metastatic prostate cancer. *Clin Cancer Res* 2000, 6:1038-1045.

54. Library Preparation for ESP [http://shark.ucsf.edu/~stas/ESP2/lib_prepare.html]

55. Kent WJ: BLAT--the BLAST-like alignment tool. *Genome Res* 2002, 12:656-664.

56. End Sequence Profiling Database [http://shark.ucsf.edu/~stas/ESP_GB/index.html]

57. Database of Genomic Variants [http://projects.tcag.ca/variation/]

58. Sharp AJ, Cheng Z, Eichler EE: Structural variation of the human genome. *Annu Rev Genomics Hum Genet* 2006, 7:407-442.

59. **Karolchik D, Kuhn RM, Baertsch R, Barber GP, Clawson H, Diekhans M, Giardine B, Harte RA, Hinrichs AS, Hsu F, et al: The UCSC Genome Browser Database: 2008 update.** ***Nucleic Acids Res*** **2007.**

60. **Zardo G, Tiirikainen MI, Hong C, Misra A, Feuerstein BG, Volik S, Collins CC, Lamborn KR, Bollen A, Pinkel D, et al: Integrated genomic and epigenomic analyses pinpoint biallelic gene inactivation in tumors.** ***Nat Genet*** **2002, 32:453-458.**

61. **Ried Lab Protocols [http://www.riedlab.nci.nih.gov/protocols]**

62. **Rae JM, Creighton CJ, Meck JM, Haddad BR, Johnson MD: MDA-MB-435 cells are derived from M14 melanoma cells--a loss for breast cancer, but a boon for melanoma research.** ***Breast Cancer Res Treat*** **2007, 104:13-19.**

Figure Legends

Figure 1: Schematic of ESP. End sequencing and mapping of tumor genome fragments to the human genome provides information about structural rearrangements in tumors. A BES pair is a *valid pair* if distance between ends mapped on the normal human genome sequence and the orientation of these ends and are consistent with those for a BAC clone insert; otherwise, the BES pair is *invalid.*

Figure 2: PCR validation of breakpoints in MCF7. (A) MCF7 clone 69F1 was sequenced and contained a small piece of chromosome 1 (purple rectangle) to chromosome 17 (yellow rectangle). Arrows on each rectangle indicate whether the fragment is oriented as in the reference genome (pointing to right) or inverted (pointing to left). PCR primers were designed to amplify the breakpoint and these primers were used to assay the other clones in the BES cluster with 69F1. Each of the other clones in the cluster are indicated as lines below 69F1 with the endpoints of the lines indicating the locations of the mapped ends relative to the ends of 69F1. The heterogeneous PCR results might result from heterogeneity of the MCF7 cells, or the existence of multiple versions of this breakpoint in MCF7 genome. (B) PCR results for the clones in (A). The expected size of the PCR fragment is 600 bp. (C) PCR validation of breakpoints in sequenced clone 37E22 from MCF7 and three additional clones in BES cluster all fusing nearby locations from chromosomes 1, 3, and 20. Two other clones have the same complex internal organization as 37E22 with four rearrangement breakpoints. However, clone 34J23 contains only one of these breakpoints suggesting that the rearrangement history of this clone is different from that of the others in the cluster.

Figure 3: Use of dual-color FISH for to validate a BT474 genomic breakpoint. End sequences from clone CHORI518_014-E04 clone were mapped to chromosomes 1 and 4. Clones RP11-692N22 and RP11- 1095F2 were selected from the human RPCI11 library because their sequences map just outside of tumor BES locations. These BACs were labeled with fluorescein and Texas Red, respectively. (Top) Two chromosomes containing a merged yellow signal indicating juxtaposition of both probes are indicated with white arrows (and labeled "a" and "b"). (Bottom) Each labeled chromosome is shown with corresponding inverted-DAPI banded chromosome, and red and green image layers. Black arrows identify the region where the red and green probes are juxtaposed to one another.

Figure 4: Recurrent rearrangement loci in the three breast cancer cell lines. (A and B) Four loci on 20q13.2-13.3 shared by MCF7 and BT474 and (C) a locus near the ERBB2 amplicon shared by BT474 and SKBR3. Colored boxes indicate the breakpoint regions for different BAC clones from MCF7 (blue), BT474 (red) and SKBR3 (green) as a custom track on the UCSC genome browser. A breakpoint region is defined as the possible locations of a breakpoint that are consistent with all the BES in the cluster; thus, shorter boxes indicate more precise breakpoint localization. Arrows give the strand of the mapped BES and thus point away from the fused region.

Figure 5: RT-PCR assays of fusion transcripts on a panel of breast cancer cell lines and normal tissues. HMEC-P1 stands for normal human mammary epithelial cells (passage 1), HMEC-P4 stands for HMEC passage 4 (higher passage). (A) RT-PCR reveals expression of DR00074 (*HYDIN* gene fusion) in 16 of 21 tested breast cancer cell lines, normal cultured human breast epithelial cells, and a wide range of normal human tissues. (B) RT-PCR validation of CN272097 a cDNA produced by a complex rearrangement on chromosome 5 fusing the SLC12A2 gene and EST AK090949. The results provide evidence for expression of the fused transcript in 5 of 21 breast cancer cell lines and in higher passage but not lower passage human mammary epithelial cells (HMEC). Note that

MDAMB435 was recently demonstrated to be derivative of the M14 melanoma cell line and not from breast [62], and the absence of the SLC12A2 fusion is this cell line is consistent with its absence is other non-breast tissues.

Figure 6: Results of SNP identification in BAC end sequences. (A) The number of high quality isolated SNPs in uniquely mapped BAC end sequences expressed per kilobase (Blue). Each tumor sample has a significantly higher rate of SNPs compared to the normal library, while the ovarian library shows a rate significantly higher than the other tumor samples. (Red) Fraction of SNPs not found in dbSNP124. The ovarian library shows significantly higher rate of these novel SNPs. (B) Mutational spectrum of SNPs for each of the samples. For C:G → T:A transitions and C:G → G:C transversions, the fraction at CpG dinucleotides is indicated in red and yellow, respectively.

Tables

Library Name	AA9	B421	CHORI-514	MCF7	PM-1	CHORI-510	CHORI-518	CHORI-520
Clinical sample designation	AA9	B421	S104	MCF-7	25-48	860-7	BT-474	SK-BR-3
Organ site	Brain	Breast	Breast	breast cancer adenocarcinoma (metastasis - pleural effusion)	Prostate metastasis	Ovarian carcinoma	ductal carcinoma	breast cancer adenocarcinoma (metastasis - pleural effusion)
Therapies applied	Radiotherapy	Chemotherapy 4 months prior to surgery (CMF)	No radiation or chemo prior to surgery	N/A	Hormone ablation, palliative radiotherapy	No therapy prior to surgery.	N/A	N/A
Patient status	Deceased	Deceased, no recurrence	No recurrence for 10 years	N/A	Deceased	Tumor recurred within 13 months	N/A	N/A
Total amount of tumor material used for library construction (mg)	100	150 (20mg effective)	100	N/A	50	200	N/A	N/A
Average clone size (± standard deviation), kb	129.1±38.3	136.4±29.2	166.1±53.2	148.0±30	N/D	149.3±28.8	179±23	154±25

Table 1: Clinical characteristics of the recurrent glioblastoma AA9, primary breast tumors B421 and S104, ovarian tumor 860, prostate metastasis 25-48 and the breast cancer cell lines MCF7, BT474, and SKBR3 used for BAC library construction. Average clone size was determined by PFGE analysis of Not1-digested DNA from 30-100 clones. (N/D means that the number was not determined, while N/A means that the number is not applicable for cell lines which can be grown in any amount and whose clinical history is not available). The presence of a large blood clot in B421 sample reduced an effective amount of tumor tissue to estimated 20 mg (out of ~150mg received from tumor bank).

	MCF7	BT474	SKBR3	Breast	Breast.2	Ovary	Prostate	Brain	Normal
Library Name	MCF7_1	CHORI-518	CHORI-520	B421	CHORI514	CHORI510	PM1	IGBR	K0241
Num mapped clones	12143	8044	7363	6972	5678	3946	3499	3238	609
Unique mapped clones	11492	7547	6950	6540	5381	3714	3296	3051	568
Valid pairs	11001	7361	6763	6376	5268	3627	3200	2984	560
Number Contigs	6323	4135	4171	4365	3450	2877	2747	2573	548
Contig coverage	0.324	0.327	0.274	0.233	0.243	0.155	0.104	0.103	0.019
Invalid pairs	491	186	187	164	113	87	96	67	8
Fraction invalid	0.043	0.025	0.027	0.025	0.021	0.023	0.029	0.022	0.014
p-value	**4.10E-04**	**0.056**	**0.032**	**0.051**	0.133	**0.080**	**0.020**	0.113	NA
Number clusters	36	26	24	2	7	2	2	0	0
Invalid pairs in clusters	164	61	64	4	24	4	4	0	0

Table 2: Results of end sequencing and mapping of each library. The fraction of invalid pairs is calculated relative to the number of uniquely mapped pairs. The p-value is the probability that the fraction of invalid pairs is the same as observed in the normal library, using a sample proportion test with pooled variance.

Sample	Clones with identified or sequenced breakpoints	Total Number of identified/sequenced breakpoints	Intragenic rearrangements	Gene:intergenic fusions	Gene:gene fusions	Intergenic:intergenic fusions
MCF7	12	36/35	3	10	19	4
BT474	6	15/6	3	2	10	0
SKBR3	8	24/8	7	4	12	1
Breast (2B421)	3	3/3	0	0	3	0
Breast (CH514)	0	-	-	-	-	-
Ovary	4	4/4	0	0	4	0
Prostate	5	5/5	0	4	1	0
Brain	3	3/3	0	3	0	0

Table 3: Summary of BAC sequencing. Breakpoints are indicated as *sequenced* if the nucleotide sequence was obtained, or *identified* if the breakpoint was localized to 3 kb subclones.

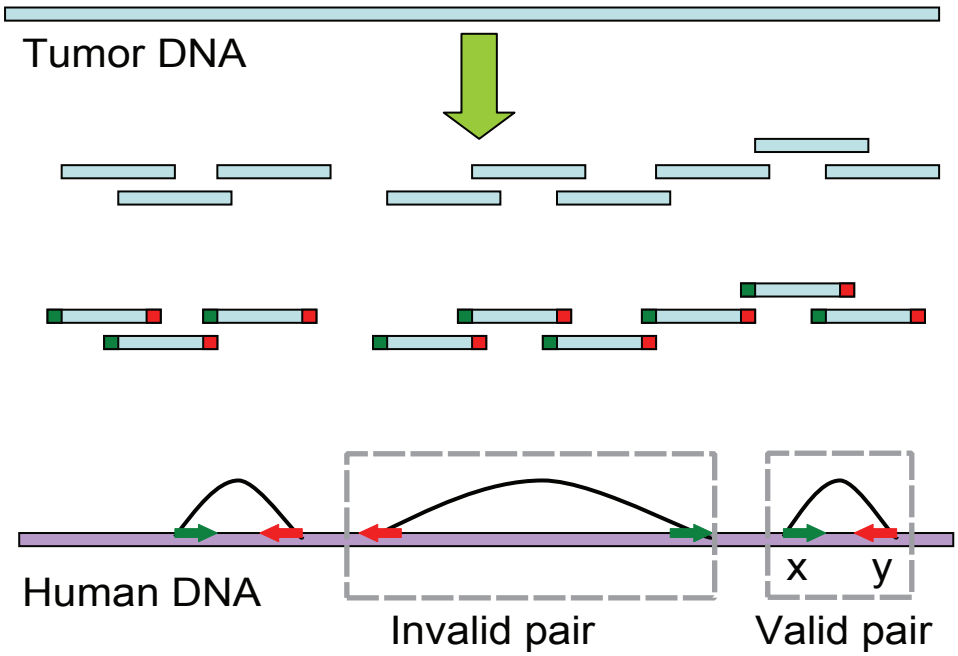

1) Clone 100-250 kb pieces of tumor genome.

2) Sequence ends of clones (500 bp).

3) Map end sequences to human genome.

Figure 1

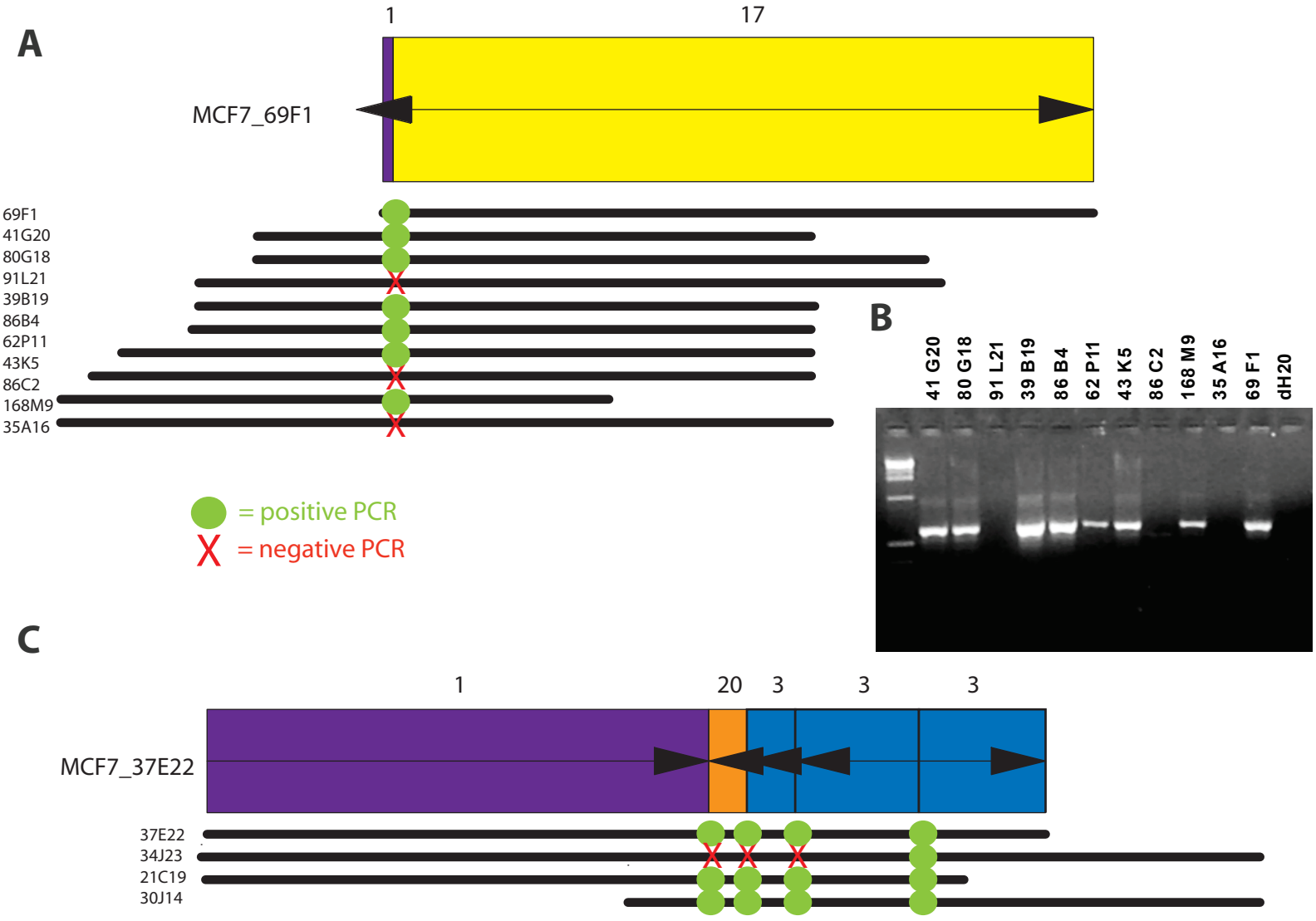
A
1
17
MCF7_69F1
69F1
41G20
80G18
91L21
39B19
86B4
62P11
43K5
86C2
168M9
35A16
= positive PCR
= negative PCR
B
41 G20
80 G18
91 L21
39 B19
86 B4
62 P11
43 K5
86 C2
168 M9
35 A16
69 F1
dH20
C
1
20
3
3
3
MCF7_37E22
37E22
34J23
21C19
30J14

Figure 2

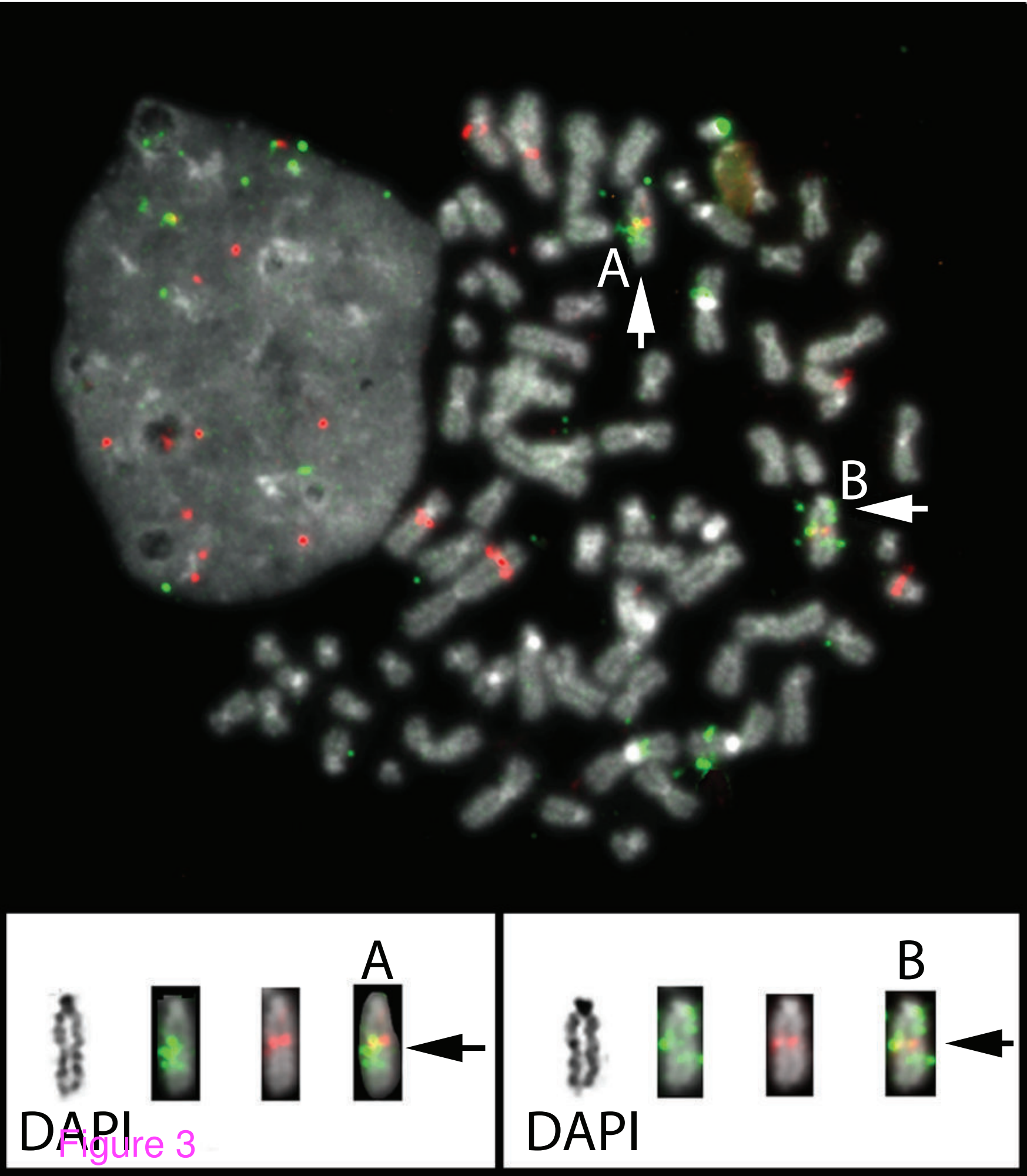

Figure 3

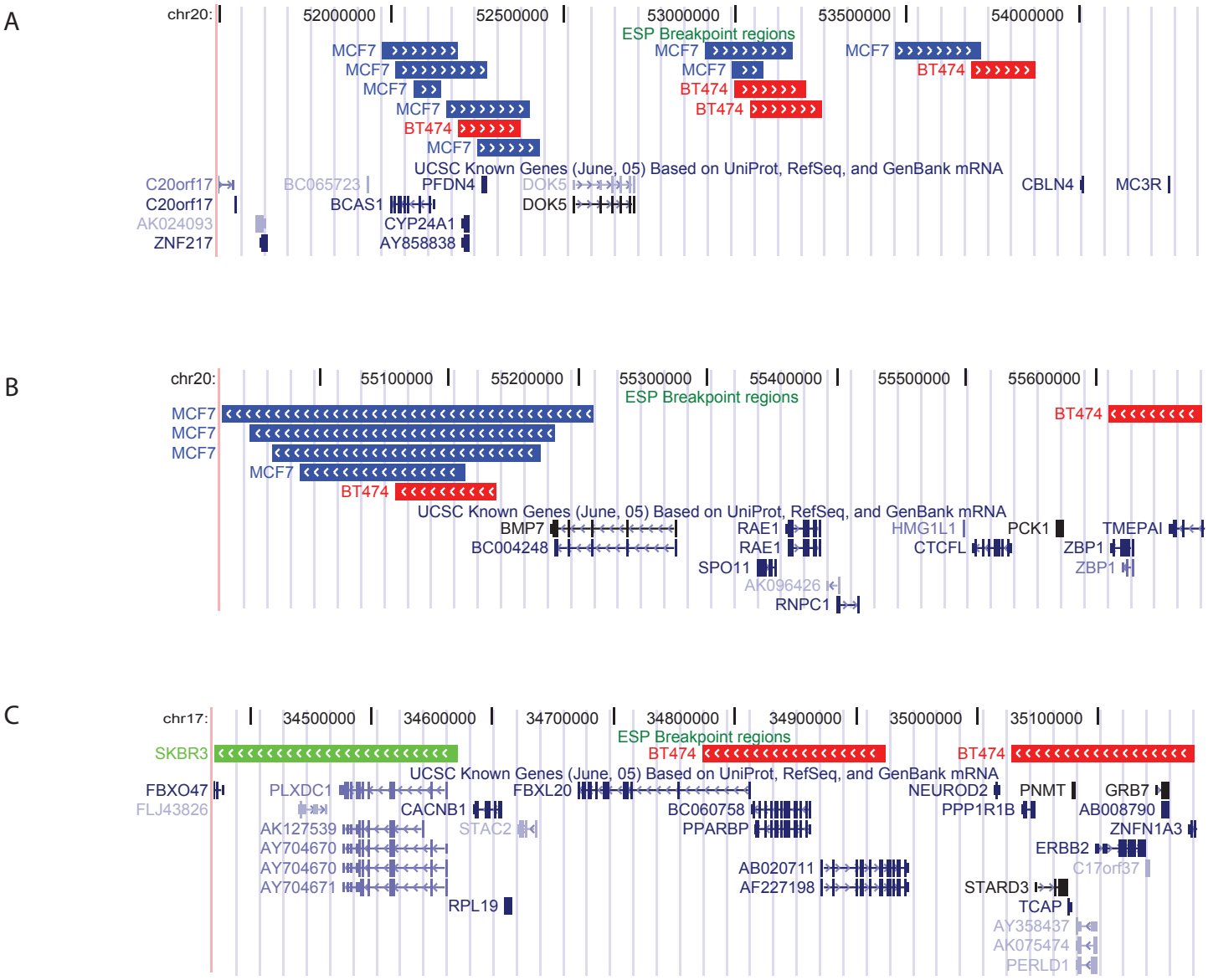
A
chr20:
52000000
52500000
53000000
53500000
54000000
ESP Breakpoint regions
MCF7
MCF7
MCF7
MCF7
MCF7
MCF7
MCF7
MCF7
BT474
BT474
BT474
BT474
UCSC Known Genes (June, 05) Based on UniProt, RefSeq, and GenBank mRNA
C20orf17
C20orf17
AK024093
ZNF217
BC065723
PFDN4
BCAS1
CYP24A1
AY858838
DOK5
DOK5
CBLN4
MC3R
B
chr20:
55100000
55200000
55300000
55400000
55500000
55600000
ESP Breakpoint regions
MCF7
MCF7
MCF7
MCF7
BT474
BT474
UCSC Known Genes (June, 05) Based on UniProt, RefSeq, and GenBank mRNA
BMP7
BC004248
RAE1
RAE1
SPO11
AK096426
RNPC1
HMG1L1
CTCFL
PCK1
TMEPAI
ZBP1
ZBP1
C
chr17:
34500000
34600000
34700000
34800000
34900000
35000000
35100000
ESP Breakpoint regions
SKBR3
BT474
BT474
UCSC Known Genes (June, 05) Based on UniProt, RefSeq, and GenBank mRNA
FBXO47
FLJ43826
PLXDC1
CACNB1
AK127539
AY704670
AY704670
AY704671
STAC2
RPL19
FBXL20
BC060758
PPARBP
AB020711
AF227198
NEUROD2
PPP1R1B
PNMT
GRB7
AB008790
ZNFN1A3
ERBB2
C17orf37
STARD3
TCAP
AY358437
AK075474
PERLD1

Figure 4

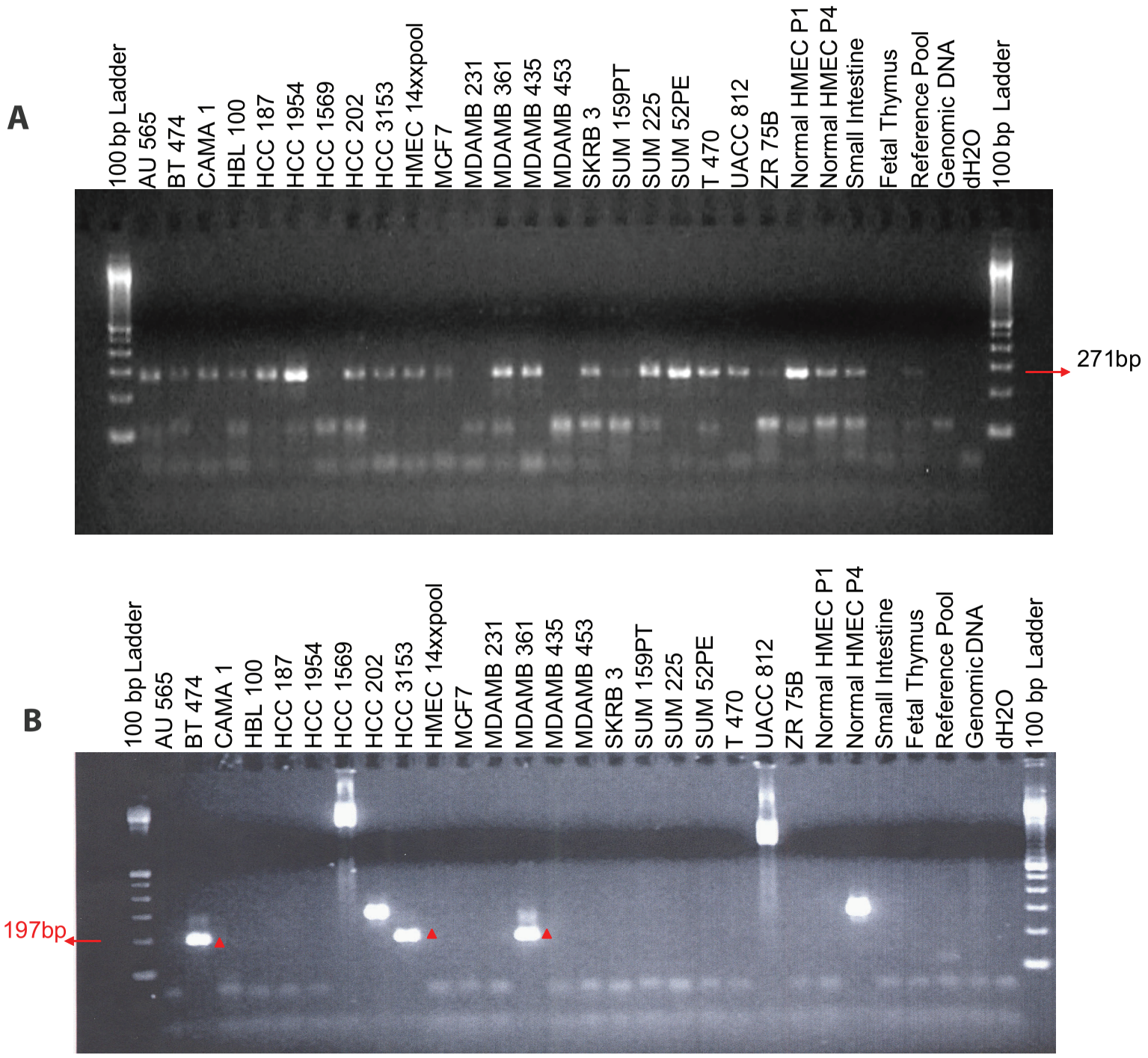
A
100 bp Ladder
AU 565
BT 474
CAMA 1
HBL 100
HCC 187
HCC 1954
HCC 1569
HCC 202
HCC 3153
HMEC 14xxpool
MCF7
MDAMB 231
MDAMB 361
MDAMB 435
MDAMB 453
SKRB 3
SUM 159PT
SUM 225
SUM 52PE
T 470
UACC 812
ZR 75B
Normal HMEC P1
Normal HMEC P4
Small Intestine
Fetal Thymus
Reference Pool
Genomic DNA
dH2O
100 bp Ladder
271bp
B
100 bp Ladder
AU 565
BT 474
CAMA 1
HBL 100
HCC 187
HCC 1954
HCC 1569
HCC 202
HCC 3153
HMEC 14xxpool
MCF7
MDAMB 231
MDAMB 361
MDAMB 435
MDAMB 453
SKRB 3
SUM 159PT
SUM 225
SUM 52PE
T 470
UACC 812
ZR 75B
Normal HMEC P1
Normal HMEC P4
Small Intestine
Fetal Thymus
Reference Pool
Genomic DNA
dH2O
100 bp Ladder
197bp

Figure 5

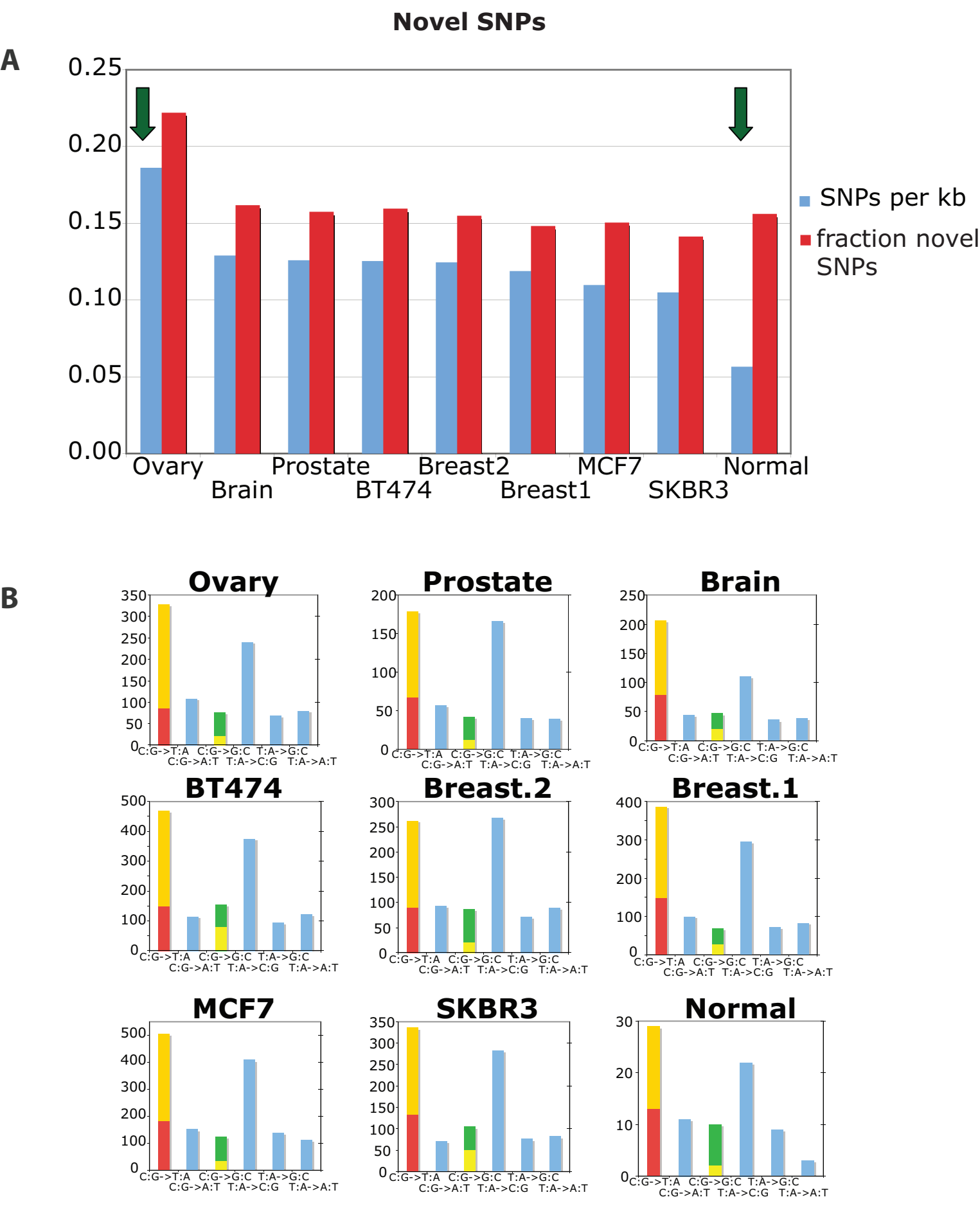
Novel SNPs
A
0.25
0.20
0.15
0.10
0.05
0.00
Ovary
Brain
Prostate
BT474
Breast2
Breast1
MCF7
SKBR3
Normal
SNPs per kb
fraction novel SNPs
B
Ovary
Prostate
Brain
BT474
Breast.2
Breast.1
MCF7
SKBR3
Normal
C:G->T:A C:G->G:C T:A->G:C
C:G->A:T T:A->C:G T:A->A:T

Figure 6